Journal of Materials Chemistry A

Accepted Manuscript

ROYAL SOCIETY OF CHEMISTRY

www.rsc.org/materialsA

Journal Name

RSCPublishing

ARTICLE

Metal Acetylacetonate Complexes for High Energy Density Non-Aqueous Redox Flow Batteries

Cite this: DOI: 10.1039/x0xx00000x

J. A. Suttil,[a] J. F. Kucharyson,[b] I. L. Escalante-Garcia,[c] P. J. Cabrera,[a] B. R. James,[a] R. F. Savinell,[c] M. S. Sanford[a] and L. T. Thompson[b,d]

Received 00th January 2012,
Accepted 00th January 2012

DOI: 10.1039/x0xx00000x

www.rsc.org/

This paper describes the design, synthesis, and fundamental characterization of a series of Cr and V acetylacetonate (acac) complexes for use in redox flow batteries (RFBs). These materials offer a significant improvement in theoretical energy density relative to state-of-the-art aqueous chemistries. A detailed assessment of the solubility, cyclic voltammetry, and charge-discharge behavior of the complexes is presented. Their solubilities in acetonitrile vary by more than four orders of magnitude based on the structure/substituents on the acac ligand. Complexes bearing acac ligands with ester substituents have solubilities of up to 1.8 M, a significant improvement over most other metal complexes that have been considered for non-aqueous RFB applications. While the acac ligand substituents have a dramatic impact on solubility, they do not, in most cases, impact the electrochemical properties of the complexes. For instance, voltammetry for all of the $V(acac)_3$ derivatives examined exhibit two quasi-reversible redox events separated by approximately 2.1 V. Charge/discharge testing in static H-Cell and laboratory-scale flow batteries yielded energy densities that were consistent with the voltammetry and coloumbic and energy efficiencies of up to 92% and 87%, respectively. Overall, these studies provide the basis for the development of structure-function relationships that could lead to new and even better performing energy storage chemistries in the future.

Introduction

Electricity accounts for approximately 40% of the energy consumed annually in the United States, and nearly 70% of this electricity is derived from non-renewable fossil fuels.[1] U.S. emissions from the 2.88 billion MWh generated from fossil fuels were 830 kg CO_2/MWh, 1.9 kg SO_2/MWh, and 0.9 kg NO_x/MWh in 2010.[2] Despite these issues and significant incentives, renewable resources were responsible for just 2.5% of net electricity generation in 2010.[2] One of the greatest challenges associated with the integration of renewables into the grid is the lack of reliable, low-cost electrical energy storage (EES) devices to deal with the mismatch between supply and demand that often arises with intermittent sources like solar and wind.[3,4,5] In addition, EES devices have the potential to increase grid stability in the event of unexpected power interruptions by providing an immediate source of stored energy.[4]

Redox flow batteries (RFBs)[4,5] have emerged as one of the most promising candidates for grid-scale energy storage. RFBs employ solutions of redox active materials. These solutions are stored in separate tanks, and the batteries can be charged or discharged by pumping the solutions through an electrochemical conversion cell.[6] The separation of these electrolytic solutions minimizes battery self-discharge, thereby providing improved efficiency when compared to other types of batteries. RFBs also offer the advantage that energy storage is decoupled from power generation.[4,6] As such, energy storage and load-leveling needs can be met independently by individually sizing the RFB storage tanks and the converters. The energy storage density (Ê) is directly proportional to three parameters: (1) the cell potential (V_{cell}), (2) the concentration of the redox active species (C_{active}), and (3) the number of electrons transferred during the redox reactions (n). A convenient figure of merit for the maximum energy stored by an RFB is shown in **Equation 1**:

$$\hat{E} = 0.5 \times V_{cell} \times C_{active} \times n \times F \quad (1)$$

Most commercial RFBs utilize aqueous solutions of transition metal salts, and state of the art systems have energy storage densities of ~25 Wh/L.[7] While progress is being made to increase the energy densities,[8], their maximum energy densities are fundamentally limited by the relatively narrow electrochemical window of water, which restricts the cell potential (V_{cell}) to ~1.2-1.6 V.[5,6,9,10] An attractive approach to

address this limitation is to develop RFBs that utilize non-aqueous solvents.[11] Acetonitrile, for example, is stable over ~5 V, which represents a nearly 4-fold improvement over the operating voltage window for water.[12] Non-aqueous solvents are more expensive than water, and can pose several safety issues (e.g., flammability and toxicity), however, these issues can be addressed with proper engineering. For example, the cost benefit ratio could improve dramatically if high energy density chemistries are demonstrated.

The use of non-aqueous solvents for RFBs was first explored by Matsuda and co-workers in the 1980s.[13, 14] These studies focused on acetonitrile solutions of transition metal bipyridine and acetylacetonate complexes. In the period following these initial investigations, reports of non-aqueous RFB chemistries have primarily focussed on transition metal complexes bearing bipyridine,[15-17] β-diketonate,[15, 18-24] bis(acetylacetone)ethylenediamine,[25] or dithiolene[26] ligands dissolved in acetonitrile and/or propylene carbonate. Polyoxometalates,[27] redox active organic molecules,[28-30] and semi-solid electrolytes[31-34] have also been explored. While many of these systems have favorable properties for flow battery applications (including reversible redox chemistries and high stabilities), they generally exhibit modest solubilities in organic solvents. To date, the most soluble transition metal complexes examined for non-aqueous RFB applications involving multiple electron transfers reach saturation at ~0.8 M in acetonitrile. Single electron transfer complexes reach 1.8 M in carbonate solvents.[26, 35] Efforts to improve solubility in both types of systems have focused almost exclusively on commercially available ligands and transition metal complexes. As a result, there have been few systematic studies of the impact of chemical structure on the solubility, electrochemical, and battery performance-relevant properties of transition metal active species in non-aqueous RFBs.

This paper describes the synthesis of a series of Cr and V acetylacetonate derivatives and a detailed assessment of their solubility, cyclic voltammetry, and charge-discharge behavior as a function of ligand structure. Most significantly, we demonstrate that the solubility of these complexes in acetonitrile can be varied by more than four orders of magnitude by tuning the ligand structures.

Results and discussion

Active Species Design and Synthesis

Our studies focused on the functionalization of chromium(III)[18] and vanadium(III)[19, 23, 24] acetylacetone (acac) complexes. Previous work has shown that the parent complexes $Cr(acac)_3$ and $V(acac)_3$ have electrochemical properties that are attractive for applications in non-aqueous RFBs. In acetonitrile, $V(acac)_3$ (**1**) has two quasi-reversible redox couples, with a potential window of 2.2 V,[19] while $Cr(acac)_3$ (**2**) offers a wider electrochemical window, albeit with less reversible redox chemistry.[18] Nevertheless, the theoretical energy storage densities for these materials remain relatively low (~12 and 40 Wh/L, respectively), due to their low solubilities in acetonitrile.

We hypothesized that systematic derivatization of the acac ligand framework could be used to tune the solubility of these Cr and V acetylacetonate complexes. This hypothesis was predicated on prior work by Yamamura, who reported that the solubility of uranium acac complexes could be modulated by replacing acetylacetone with other commercially available 2,4-disubstituted acac derivatives.[21] In the current study, we targeted a diverse set of 2,4- and 3-substituted acac ligands bearing polar functional groups (e.g., bromine, nitro, amino, ester, ether, and cyano substituents), as we hypothesized that these would enhance solubility in polar aprotic organic solvents.[28]

Our initial focus was on the synthesis of derivatives of $Cr(acac)_3$. Despite the modest reversibility of the redox chemistry in this system, derivatives of $Cr(acac)_3$ are straightforward to prepare. Furthermore, these Cr complexes are air and moisture stable, enabling facile manipulation and purification. Notably, we also anticipated that we might observe variations, albeit subtle, in the electrochemical properties of the complexes as a function of ligand substitution. As highly soluble Cr derivatives were identified, we then undertook the more challenging synthesis of their vanadium analogues, which generally show more reversible electrochemistry.

Complexes **3-6** (**Figure 1a**) were prepared by the reaction of $Cr(acac)_3$ with electrophiles, using previously reported procedures.[36-41] Complexes **7-9** (**Figure 1b**) were synthesized through a disproportion reaction between $Cr(acac)_3$ and 1,3-diphenyl-1,3-propandione.[36] This transformation afforded a mixture of products **7-9** that could be readily separated via column chromatography on silica gel. Finally, complexes **10-15** (**Figure 1c**) were accessed in two steps. First, the 3-substituted ligands were synthesized by conjugate addition of acetylacetone with a diverse range of acrylate derivatives.[42] Next, deprotonation of the ligand with sodium hydride followed by introduction of $CrCl_3(thf)_3$ or $VCl_3(thf)_3$ produced the corresponding Cr or V adducts. All of the metal complexes were characterized by elemental analysis and mass spectrometry. In addition, X-ray crystal structures of **6**, **8**, and **9** were obtained (see Supporting Information).

Solubilities

The solubilities of complexes **1-15** in acetonitrile were measured using a UV-Visible spectroscopic method (**Figure 2**, **Tables 1** and **2**). The parent $V(acac)_3$ (**1**) and

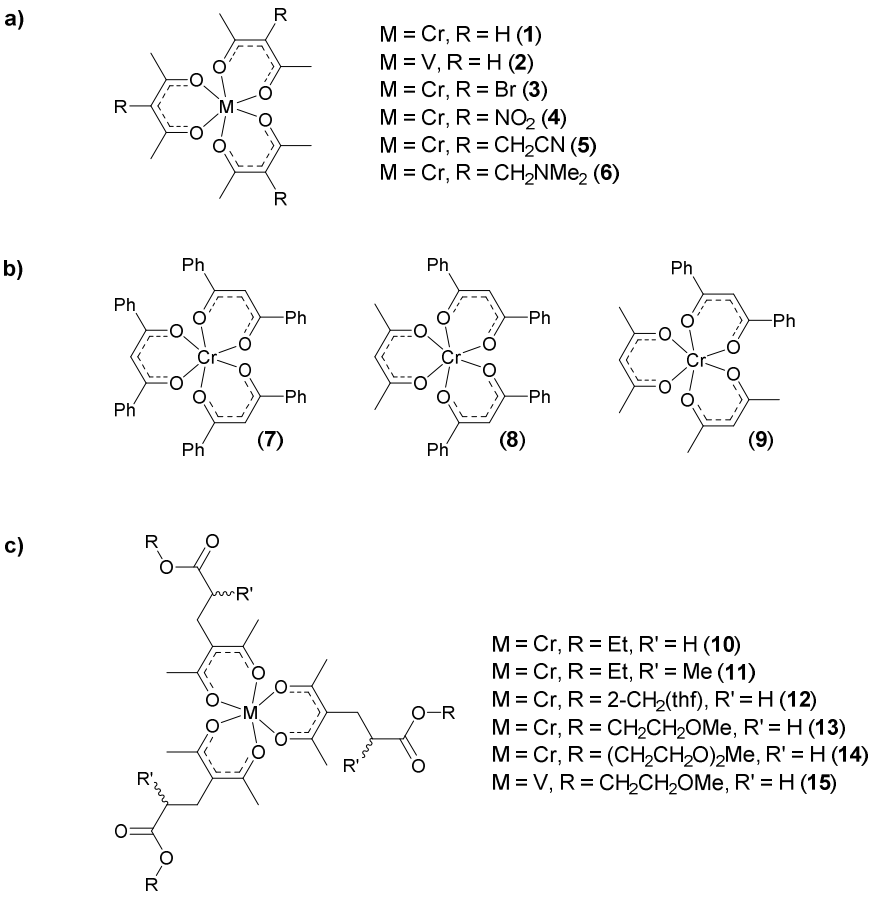

Figure 1: a) Previously reported complexes assessed herein (1 – 6). b) Phenyl-substituted chromium(III) acetylacetonate complexes (7 - 9) through ligand disproportionation. c) Ester functionalized chromium(III) and vanadium(III) acetylacetonate complexes (10 – 15).

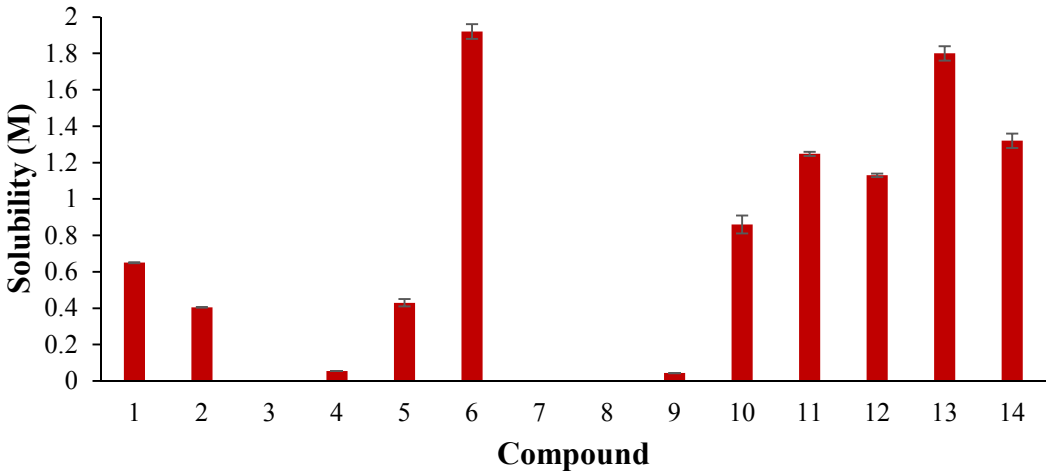

Figure 2. Solubilities for complexes 1 – 13 and 15 in acetonitrile as assessed using UV-Visible spectrophotometry.

Table 1. Solubility and electrochemical data for chromium(III) and vanadium(III) acetylacetonate complexes 1-6 and 10-15.

Complex	Solubility [M]	M(I)/M(II) Couple[a]	M(II)/M(III) Couple[a]	M(III)/M(IV) Couple[a]	M(IV)/M(V) Couple[a]
1	0.65	-	-1.78 (0.98)	0.41 (1.03)	-
2	0.404	-2.51 (0.41)	-2.24 (0.59)	1.17 (3.95)	1.55 (1.34)
3	0.002	-2.17 (0.20)	-1.75 (0.16)	1.28 (3.71)	1.57 (3.11)
4	0.05	-2.44 (0.77)	-	-	-
5	0.43	-2.23 (0.36)	-1.96 (0.32)	1.27 (3.84)	1.61 (2.27)
6	1.92	-2.45 (0.57)	-2.21 (0.59)	-	-
10	0.86	-2.42 (0.27)	-2.19 (0.34)	0.98 (2.60)	1.39 (3.51)
11	1.25	-	-2.32 (0.19)	0.97 (2.94)	1.42 (4.07)
12	1.13	-2.42 (1.33)	-2.18 (0.45)	0.99 (3.29)	1.35 (2.47)
13	1.8	-2.41 (2.17)	-2.19 (0.30)	0.97 (2.66)	1.34 (3.81)
14	-	-2.43 (0.75)	-2.19 (0.42)	0.99 (2.96)	1.38 (2.66)
15	1.32	-	-1.96 (0.97)	0.15 (1.02)	-

[a)] Standard potentials (measured vs Ag/Ag^+) identified using cyclic voltammetry of solutions comprised of each complex with 0.1M $TBABF_4$ in acetonitrile. Concentrations of complexes varied based on solubility and the values can be found in the Supplementary Information. Values in parentheses indicate ratios of the cathodic and anodic peak heights (i_c/i_a).

Table 2. Solubility and electrochemical properties for chromium(III) complexes 1 and 7 – 9.

Complex	Solubility [M]	Redox Couple 1[a)]	Redox Couple 2[a)]	Redox Couple 3[a)]	Redox Couple 4[a)]	Redox Couple 5[a)]
2	0.404	-2.42 (0.28)	-2.19 (0.34)	0.98 (2.60)	1.39 (3.51)	-
7	5.7×10^{-5}	-2.46 (0.79)	-2.13 (0.75)	-1.63 (1.01)	1.23 (7.86)	1.62 (2.29)
8	7.99×10^{-4}	-2.19 (1.09)	-1.69 (1.07)	1.20 (7.17)	1.61 (2.60)	-
9	0.043	-2.86 (0.25)	-1.73 (0.85)	1.22 (5.76)	1.68 (1.31)	-

[a] Standard potentials (measured vs Ag/Ag^+) identified using cyclic voltammetry of solutions comprised of each complex with 0.1M $TBABF_4$ in acetonitrile. Concentrations of complexes varied based on solubility and the values can be found in the Supplementary Information. Values in parentheses indicate ratios of the cathodic and anodic peak heights (i_c/i_a).

$Cr(acac)_3$ (**2**) have solubilities of 0.65 and 0.40 M, respectively. These values are consistent with those reported in the literature.[18, 19] The incorporation of Br, NO_2, and phenyl substituents on the acetylacetonate ligand has a deleterious effect on the solubility of the corresponding Cr complexes (**3**, **4**, and **7-9** have solubilities of 0.002, 0.05, and 5.7×10^{-5} to 0.043 M, respectively). Conversely, incorporation of the $–CH_2CN$ moiety (**5**) results in a small increase in solubility (to 0.43 M). The addition of a $–CH_2NMe_2$ group at the 3-position (**6**) dramatically enhances the solubility (to 1.92 M);[39] however, this ligand suffers from redox instability (*vide infra*). Finally, complexes bearing ester-substituted ligands (**10-15**) show significant enhancements in solubility relative to the parent $M(acac)_3$. The improvements in solubility can be attributed to both the reduction in crystallinity of these molecules, as they exist at room temperature as highly viscous tars or oils, and the increased incorporation of polar functional groups, such as esters and ether, which are more miscible with polar solvents such as acetonitrile. Most dramatically, complexes bearing the 2-methoxyethyl-substituted ester (**13** and **15**) are highly viscous oils with solubilities of 1.8 M and 1.32 M in acetonitrile, respectively. These solubilities are up to ~3-fold higher than those for the parent $Cr(acac)_3$ and $V(acac)_3$. Overall, these studies show that systematic substitution of the acac ligands leads to complexes with solubilities in acetonitrile ranging over four orders of magnitude (5.7×10^{-5} to 1.92 M). Furthermore, these investigations provide insights into the influence of various functional groups on solubility. We anticipate that this latter information will be more broadly applicable to the development of novel redox active molecules for non-aqueous RFBs.[43, 44]

The high solubility and viscous nature of complex **13** led us to hypothesize that further extension of the ether chain would result in a metal complex that is a liquid at room temperature. Indeed, the 2-(2-methoxyethoxy)ethyl-substituted ester complex **14** is a high-viscosity liquid, and the addition of acetonitrile merely serves to dilute this complex. As such, a solubility determination is not meaningful. This molecule (and derivatives thereof) holds promise for the development of high energy density, solvent-free chemistries for RFBs and will provide the basis for future work.

Finally, we compared the solubilities of complexes **2** and **13** in dimethylcarbonate (DMC) and tetraethylene glycol dimethyl ether (TEGDME), solvents that are often considered for RFBs.[33] As shown in **Figure 3**, both complexes are significantly less soluble in these solvents compared to in acetonitrile. However, in all cases, the ester functionality imparts an approximately 4-fold enhancement in solubility relative to the parent complex **2**. The solubility measurements are for the neutral complexes. Preliminary bulk electrolysis results show the solubility of complex **1** changes by less than 25% when charged. This is a significant decrease and future work will investigate the effects of state of charge in greater detail.

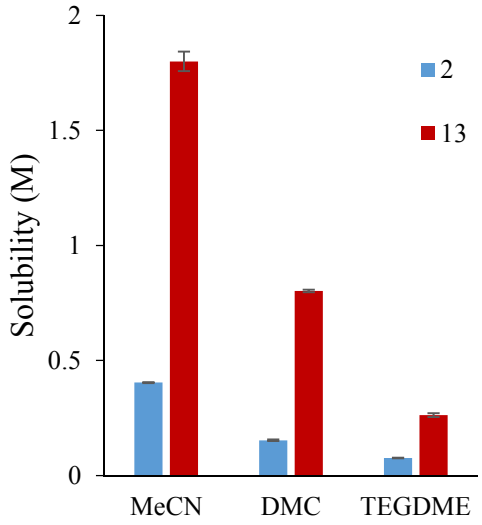

Figure 3. Solubilities of complexes 2 (blue) and 13 (red) in acetonitrile (MeCN), dimethylcarbonate (DMC) and tetraethylene glycol dimethyl ether (TEGDME).

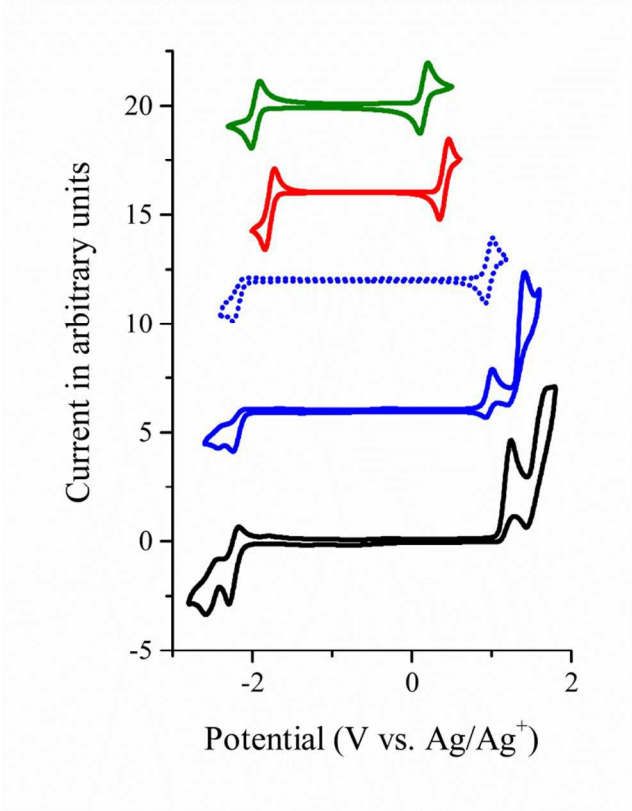

Figure 4. Cyclic voltammograms of 2 (black), 13 (2 redox couples - dashed and 4 redox couples - solid blue), 1 (red) and 15 (green). Solutions comprised of 0.01M active species and 0.1M $TBABF_4$ in acetonitrile.

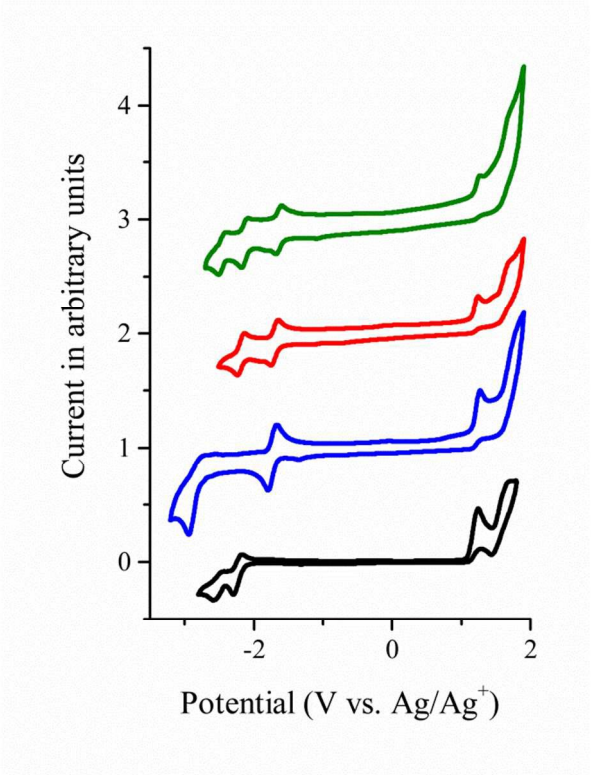

Figure 5. Cyclic voltammograms of 0.01M 2 (black), 0.00014M 7 (green), 0.001M 8 (red) and 0.001M 9 (blue) with 0.1M $TBABF_4$ in acetonitrile.

Electrochemical Properties

The energy density of a RFB is directly proportional to its operating potential (V_{cell}). In addition, the reversibility of each redox couple is extremely important for battery performance, as poor reversibility will limit battery cycle-life. Cyclic voltammetry (CV) was used to determine the potentials and reversibilities for redox couples associated with all of the new complexes. A time semi-derivative method was used to deconvolute the CVs, and the reversibility of each couple was quantitatively assessed using the current peak height ratios (i_c/i_a).[45-47] Peak height ratios near unity are consistent with high redox reversibility. Representative cyclic voltammograms are shown in **Figure 4**. The results are summarized in **Table 1**.

The parent complex Cr(III) acetylacetonate (**2**) shows four redox couples with relatively poor reversibility (i_c/i_a ranging from 0.41 to 3.95).[18] Electrochemical characterization of complex **4** shows no redox couples at positive potentials, while

only one negative couple is apparent, with very slow kinetics (~300 mV peak separation). A previous report of the electrochemical behavior of complex **4** made no mention of slow kinetics; furthermore, an additional redox couple was mentioned in the prior report but was not observed in the current experiments.[41] Complex **5** shows similar electrochemical behavior to complex **2** at negative potentials, but there is evidence of side reactions at positive potentials. These features are likely due to ligand detachment and/or degradation. The other Cr(III) complexes (**3, 6, 10-14**) show electrochemical properties very similar to those of the parent complex **2**, with small shifts in the potentials from complex to complex. With some of the ester functionalized ligands, the $Cr^{III/IV}$ couple was slightly more reversible (**Table 1**, *cf.* entries 2 & 11).

A previous study of **7** using polarography showed that this complex displays extra redox couples relative to Cr(III) acetylacetonate, which we hypothesize are due to ligand non-innocence.[41] The heteroleptic complexes **8** and **9** allowed us to assess the extent of this effect. The cyclic voltammetry (**Table 2**, **Figure 5**), shows a direct correlation between the number of 1,3-diphenyl-1,3-propandione ligands in the metal complex and the number of additional redox events. However, the incorporation of each non-innocent phenyl-moiety has an incremental deleterious effect on complex solubility, with complex **7** exhibiting the lowest solubility reported herein. Nevertheless, ligand non-innocence provides a potentially attractive method for increasing RFB energy density if more soluble ligand motifs can be identified.[48]

Previous work has shown that $V(acac)_3$ (**1**) has significantly more reversible electrochemistry than its Cr analogue (**2**).[19, 23, 24] Similarly, the oxidation and reduction peaks for V complex **15** have i_c/i_a values very close to unity (-1.96 V = 1.02 and 0.15 V = 0.97), while those for the Cr analogue **13** are not close to unity (-2.41 V = 2.17, -2.19 V = 0.30, 0.97 V = 2.66 and 1.34 V = 3.81). We note that in a smaller voltage window, the first oxidation couple for **13** exhibits improved reversible (i_c/i_a = 0.96) (**Figure 4**). **Figure 4** also shows that the redox couples for **15** are shifted to more negative potentials by ~260 mV relative to those of $V(acac)_3$ (**1**). Despite this shift, the available electrochemical windows (i.e., possible battery cell potentials) for **1** and **15** are nearly identical, at 2.19 and 2.11 V, respectively.

Table 3. Diffusion coefficients for complexes 1, 2, 13 and 15 in acetonitrile.

Complex	D_O x10^{6} [a] [cm^2/s]	D_O x10^{6} [b] [cm^2/s]
1	1.8–2.9[19]	5.2-6.2
2	0.5-0.62[18]	6.8-8.2
13	-	3.6-4.4
15	-	3.9-4.7

[a] Literature value; [b] This work

Another important characteristic for the active species in an RFB is the diffusion coefficient. The diffusion coefficient will impact the power density that can be achieved. Adding substituents to the acetylacetonate ligand is expected to negatively impact the diffusion coefficient, based on the Stokes-Einstein equation.[49] This could result in reduced transport rates and could ultimately limit power densities for the associated RFBs.[49] Diffusion coefficients for complexes **1**, **2**, **13**, and **15** (see **Table 3**) in acetonitrile were obtained from cyclic voltammograms at varying scan rates. The data were fit to the Randles-Sevcik equation (**Equation 2**).

$$i_p = 2.687 \times 10^5 \times n^{3/2} \times A \times D^{1/2} \times C_o \times \nu^{1/2} \quad (2)$$

Here, i_p is the peak current for the oxidation or reduction reaction, n is the number of electrons transferred (one in this case), A is the area of the electrode, D is the diffusion coefficient of the reacting species, C_o is the bulk concentration of the active species, and ν is the scan rate. This equation assumes reversible reactions, so slow scan rates and redox couples with peak height ratios close to unity were used. Scan rates of 10-100 mV/s were utilized for all complexes, and plots of i_p vs. $\nu^{1/2}$ were linear in all cases. The linearity indicates a diffusion-controlled redox process, and the slope was used to calculate the diffusion coefficients. As shown in **Table 3**, the diffusion coefficients for **13** and **15** are lower than those for **1** and **2**, respectively. This is expected based on the larger substituents on the ligands of **13** and **15** compared to **1** and **2**.[49] However, all of the values are within the same order of magnitude and are expected to be adequate for RFB applications.[6]

Charge-Discharge Characteristics

Cr complex **13** and V complex **15** displayed the most attractive combination of solubility and electrochemical properties in acetonitrile, and were therefore evaluated in charge/discharge experiments. In each experiment, the same complex was used as both the catholyte and anolyte to limit the deleterious effects of cross-over.

Preliminary experiments were carried out in an H-cell. **Figure 6a** shows charge/discharge results for a 0.05 M acetonitrile solution of complex **13** with 0.5 M of tetrabutylammonium tetrafluoroborate added as the supporting electrolyte. **Figure 6b** shows the charge/discharge results for **15** under similar conditions. Constant current densities of 0.21 mA/cm^2 and 0.021 mA/cm^2 were used for charging and discharging, respectively. A lower discharging current was used to limit overpotentials and ensure the cell was completely discharged. Cut-off charging potentials of 3.5 V and 2.4 V were used for complex **13** and complex **15**, respectively, with a discharging potential of 1.0 V for both complexes. The charging potentials were selected based on the measured cell resistance of 206 Ω, which would result in a 0.1 V overpotential. This overpotential is primarily due to the large separation between the two electrodes, with contributions from membrane and solution resistances.

Solutions containing chromium complex **13** were cycled more than 20 times. In a typical cycle **(Figure 6a)**, this

complex charges in ~0.6 hrs, which correlates well with the one electron transfer predicted by CV. The lack of a discernible voltage plateau during discharge is indicative of the poor reversibility of the complex. The cell stabilized after six cycles at coulombic efficiencies of ~55% and energy efficiencies of ~25%. These values are similar to those reported previously for $Cr(acac)_3$ (**2**) in an H-cell (53-58%, and 21-22%, respectively),[18] and are consistent with the similar electrochemical behaviour of complexes **2** and **13**, as assessed

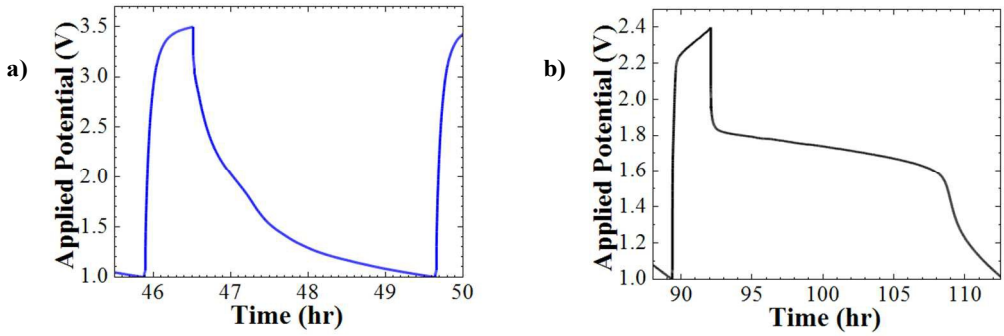

Figure 6. H-Cell charge/discharge experiments of 0.05 M solutions of (a) chromium complex 13 (cycle 7) and (b) vanadium complex 15 (cycle 4) with 0.5M $TBABF_4$ in acetonitrile. The first stable cycle of each experiment is shown.

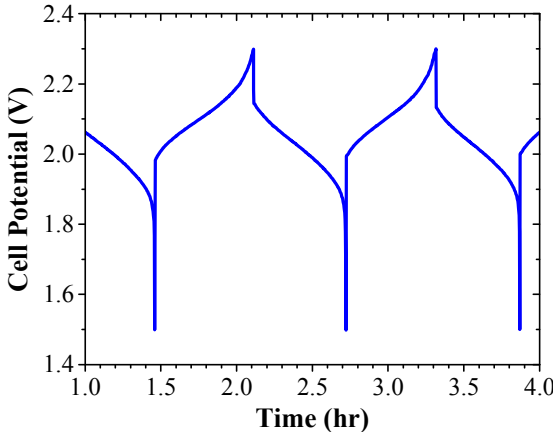

Figure 7. Flow battery charge/discharge cycles of 0.1 M vanadium complex 15 with 1 M $TEABF_4$ in acetonitrile at 10 mA/cm^2 in a RFB cell. Cycles 2 and 3 are shown. Flow rate: 25 ml/min. Room temperature.

by CV. The modest coulombic and energy efficiencies can be attributed to the irreversible nature of the electrochemistry.

Figure 6b shows that vanadium complex **15** charges in ~3 hrs which correlates well with the electrochemistry indicated by the CV. In contrast to complex **13**, this system shows a discharge plateau at ~1.8 V, which again correlates to the CV when overpotentials are taken into account. The cell stabilizes after the first three cycles at coulombic efficiencies of ~76% and energy efficiencies of ~52%. These results are similar to those obtained with the parent $V(acac)_3$ (**1**), which was reported to have coulombic efficiencies of 70-73% and an energy efficiency of 34%.[19, 23] The performance of cells containing the V complexes are superior to those for the Cr complexes due to the increased reversibility of the redox couples with V.

Given results from the H-Cell experiments, the performance of vanadium complex **15** was further investigated in a laboratory-scale flow-through electrode configuration RFB cell. A 0.1 M solution of complex **15** in acetonitrile with 1 M tetraethylammonium tetrafluoroborate as supporting electrolyte was used as both the catholyte and the anolyte. The non-aqueous vanadium RFB cell was initially charged to 75% of the theoretical state of charge (SOC) at 10 mA/cm^2. The open circuit cell potential (OCV_{cell}) and electrochemical impedance were measured at the end of the first charge. The RFB cell resistance was ~1.75 □·cm^2 which was much lower than that measured for the H-type cell. Thus, higher charge/discharge current densities were employed than were possible with the H-Cell. Charge/discharge cycles were performed at 10 mA/cm^2, with cut-off charging and discharging potentials of 2.3 V and 1.5 V, respectively. The vanadium RFB cell stabilized during the first C/D cycle. Overall, the cycles exhibited a single charging potential curve starting at ~2.0 V and a discharging potential curve at ~2.1 V, as shown in **Figure 7**. These results are in good agreement with the potential window predicted for **15** from the CV experiments (2.1 V). The OCV_{cell} of the vanadium RFB system was 2.17 V at the end of the first charge. The RFB cell was initially charged up to a 75% SOC; thus, a higher OCV_{cell} was expected. A cell potential of 2.1 V would correspond to a 50% SOC.

The average coulombic and energy efficiencies for the vanadium RFB cell were ~92% and ~87%, respectively, for the first 12 charge/discharge cycles. The coulombic efficiency losses may be due to (a) the loss of active species via side reactions or (b) crossover of vanadium species through the TEA-Nafion membrane. The degradation of $V(acac)_3$ due to side reactions was reported previously.[22,47] The energy performance of complex **15** is comparable with that reported for $V(acac)_3$, using a similar flow cell design.[50] The reported coulombic and energy efficiencies for 0.1 M $V(acac)_3$ were ~90% and ~83%, respectively, at 10 mA/cm^2.[50]

Conclusions

This paper describes the design and synthesis of a series of Cr and V acac complexes, and a detailed assessment of their solubility, electrochemistry, and charge-discharge behavior as a function of ligand structure. We demonstrate that the solubility of these complexes in acetonitrile can be varied by more than four orders of magnitude by tuning the ligand structures. In particular, complexes bearing ligands with ester substituents (**13** and **15**) show high solubilities in three common non-aqueous RFB solvents: acetonitrile, dimethylcarbonate, and tetraglyme. The solubilities of **13** and **15** in acetonitrile represent 450% and 200% enhancements, respectively, compared to the corresponding $M(acac)_3$ parent complexes. Electrochemical and charge-discharge studies show that **13** and **15** have electrochemical properties that are similar to the parent $M(acac)_3$ species. In static H-cell charge/discharge experiments, coulombic efficiencies of ~55% were achieved for **13** with 0.5 M $TBABF_4$ in acetonitrile, while coulombic efficiencies of ~76% were achieved for **15** under the same conditions. In an initial test of a laboratory scale prototype flow battery test with 0.1 M of **15**, we demonstrated coulombic and energy efficiencies of 92% and 87%, respectively, with operating current densities of 10 mA/cm^2. Flow cell experiments with higher concentrations of the active species would be required for further scale-up. Likewise, further optimization of the reversibility, potential limits, membranes, and electrode materials should allow the vanadium chemistry to approach the theoretical energy density predicted for saturated solutions of **15** (37.3 Wh/L). This will be the focus of our future work. Furthermore, the studies described herein provide a foundation for the rational design of novel active species with further enhancements in solubility and electrochemical properties that should ultimately surpass aqueous RFB technologies.

Experimental

General

All manipulations were performed under a nitrogen atmosphere using standard Schlenk techniques or in a nitrogen-filled MBraun glovebox unless otherwise stated. ^{1}H and ^{13}C NMR spectra were recorded using Varian VNMRS 700 and MR400 spectrometers with $CDCl_3$ as the solvent. ^{1}H and ^{13}C NMR spectra were recorded at room temperature and are reported in parts per million relative to the residual solvent peak. Mass spectra were measured using an Agilent Q-TOF mass spectrometer or Waters (VG Analytical) 70-250-S magnetic sector mass spectrometer. Elemental analyses were performed by Atlantic Microlab, Inc. Infrared spectra were recorded on a Perkin-Elmer Spectrum BX Ft-IR spectrometer employing an ATR attachment. UV-Visible measurements were collected using a Shimadzu UV-1601 UV-Visible spectrophotometer. Melting points were recorded on Mel-Temp 3.0 and are uncorrected. For synthetic chemistry, anhydrous diethyl ether, tetrahydrofuran and dichloromethane were prepared by passage through an Innovative Technologies solvent purification system and stored under an inert atmosphere. Anhydrous acetonitrile was purchased from Alfa-Aesar and used without further purification. For cyclic voltammetry and charge/discharge experiments, anhydrous acetonitrile (99.8 %) and tetrabutylammonium tetrafluoroborate (99.0 %) were purchased from Sigma Aldrich and used as received. The molecules 2-(2-methoxyethoxy)ethyl acrylate,[51] ethyl 4-acetyl-5-oxohexanoate,[52] tris(3-bromo-2,4-pentanedionato)chromium(III) (**3**),[38] tris(3-nitro-2,4-pentanedionato)chromium(III) (**4**),[37] tris(3-cyanomethyl-2,4-pentanedionato)chromium(III) (**5**)[39] and tris(3-*N,N*-dimethylaminomethyl-2,4-pentanedionato)chromium(III) (**6**)[39] were prepared according to the literature procedures. Preparation of the remaining ligands is discussed in the supporting information. All other reagents and solvents were obtained from commercial sources and were used without further purification.

Solubility Determination

Stock solutions of the desired complex were prepared in acetonitrile, in triplicate, from which standard solutions were prepared by serial dilution. Each sample used for solubility testing was analysed by PXRD before and after generation of the saturated solution to assess the solid form of the material relevant to the solubility measurement. UV-Vis spectra of the most concentrated stock solution was recorded on a Shimadzu UV-1601 UV-Visible spectrophotometer and used to determine a suitable wavelength for absorbance measurements. Absorbances of the standard solutions were then measured at the determined wavelengths and used to prepare an absorbance versus concentration calibration curve. For solids, saturated solutions were prepared by portion-wise addition of the desired complex to 300 µL of acetonitrile with stirring until a persistent suspension resulted. For viscous tars, 300 µL of acetonitrile was added to the product, and the mixture was shaken until no further material dissolved. In all cases, the solution was then filtered through cotton wool to remove any undissolved material, and three aliquots were diluted in acetonitrile to afford absorbances within the range of the calibration curve.

Cyclic Voltammetry

Cyclic voltammetry was performed using a PGSTAT302N Autolab Potentiostat and a 600D CH Instruments Potentiostat, for each complex to obtain the electrochemical window, standard potentials, and approximate reversibility. A 10 mL, three electrode electrochemical cell, fabricated in-house, was used for these experiments. The three electrodes consisted of a 0.07 cm^2 glassy carbon disk working electrode (BASi), a Ag/Ag+ quasi-reference electrode (BASi) filled with 0.01 M silver tetrafluoroborate in acetonitrile (Sigma Aldrich), and a 23 cm long platinum wire counter electrode (ALS). The working electrode was polished using 9 and 0.3 µm aluminum oxide polishing paper (Fiber Instrument). All solutions were prepared inside an Ar-filled MBraun glove box, then transferred to the

electrochemical cell and sparged with N_2 for 10 minutes. The cell was then sealed and a nitrogen headspace was maintained for the duration of the experiment. During analysis, the current peak height ratios (i_c/i_a) were obtained using a time semi-derivative (deconvolution).

Charge-Discharge Experiments

Charge/discharge experiments were performed in an H-cell using a Maccor 4000 Series Battery Tester. The constant charging and discharging currents were 0.21 and 0.021mA/cm^2, respectively. The H-cell (Adam's & Chittenden) included half cells that were separated by a Neopsepta AHA membrane (Ameridia). These membranes were pre-conditioned in 0.1 M tetrabutylammonium tetrafluoroborate (Aldrich) in acetonitrile for at least 24 h. The cell contained two ~6.4 cm^2 graphite plate electrodes (McMaster Carr) and two PTFE micro-stir bars (Fisher). The catholyte and anolyte each consisted of 5 ml of a solution of 0.05M of the redox active complex with 0.5 M tetrabutylammonium tetrafluoroborate (Aldrich) dissolved in anhydrous acetonitrile (Fisher). For complex **13**, cutoff potentials of 3.5 and 1.0 V were used. For complex **15**, cutoff potentials of 2.4 and 1.0 V were used. Electrochemical Impedance Spectroscopy (EIS) was carried out using a PGSTAT302N Autolab Potentiostat at frequencies ranging from 0.1 Hz-100 kHz at the open cell potential using an AC potential perturbation of 10 mV. The RFB cell resistance was determined from the intercept of the real part of the impedance at high frequency. The EIS and charge/discharge experiments were performed inside an Ar-filled glove box.

A laboratory-scale prototype redox flow battery system with a standard flow-through electrode configuration (RFB) for electrolyte flow was used. The RFB system used in this study was reported previously[50]. Briefly, the RFB cell consisted of graphite felt SGL GFA 3.0 (3 mm thickness, SGL group) electrodes with a geometric area of ~5.65 cm^2. A tetraethylammonium cation (TEA^+) exchanged Nafion® 1035 membrane (EW of 1000 g/mol, 89 □m nominal thickness, Alfa-Aesar) was employed as the separator. The TEA^+-form Nafion membrane was prepared as reported elsewhere[50]. After cell assembly, the electrode compression was approximately 20%. Prior to cell assembly, the electrodes were soaked in the test electrolyte for 2 hr. The catholyte and anolyte each consisted of 25 ml of a solution of 0.1 M vanadium complex **15** with 1 M tetraethylammonium tetrafluoroborate (99%, Aldrich) dissolved in anhydrous acetonitrile. The electrolyte was delivered to each cell compartment at 25 ml/min by means of a peristaltic pump (Masterflex Mod. 77800, Cole-Parmer®) with two heads. Charge/discharge battery cycles were performed at constant current density of 10 mA/cm^2 with cut-off potentials between 1 V and 2.3 V. The EIS was carried out at frequencies ranging from 0.1 Hz-250 kHz at the open cell potential bias using an AC potential perturbation of 10 mV. Before EIS measurements, the RFB cell was resting at the open circuit cell potential for 1.5 min. The RFB cell resistance value is reported as the intercept of the real part of the impedance at high frequency. A Solartron SI 1287A potentiostat/galvanostat coupled with a Solartron 1260 impedance/gain phase analyzer were employed to conduct the battery cycle testing and EIS measurements. The RFB cell was assembled and tested under a N_2-controlled atmosphere.

Acknowledgements

Research described in this paper was supported by a grant from the National Science Foundation, Sustainable Energy Pathways Program (NSF-1230236). JAS also thanks the University of Michigan Phoenix Memorial Energy Institute for a Partnerships for Innovation in Sustainable Energy Technologies (PISET) fellowship. The authors gratefully acknowledge Jeff W. Kampf for the X-ray crystallography studies, as well as Paul Rasmussen and Adam Matzger for helpful discussions.

Notes and references

[a] University of Michigan, Department of Chemistry, 930 North University Avenue, Ann Arbor, Michigan, 48109, USA.
[b] University of Michigan, Department of Chemical Engineering, 2300 Hayward Street, Ann Arbor, Michigan, 48109, USA.
[c] Case Western Reserve University, Department of Chemical Engineering, A. W. Smith Building, Cleveland, Ohio, 44106, USA.
[d] University of Michigan, Department of Mechanical Engineering, 2350 Hayward Street, Ann Arbor, Michigan, 48109, USA.

Electronic Supplementary Information (ESI) available: Ligand synthesis, complex synthesis, NMR spectra, solubility measurements, X-ray structure determination, powder X-ray diffraction patterns, cyclic voltammograms and Randles-Sevcik plots. See DOI: 10.1039/b000000x/ CCDC 992728, 992729 and 992730 contain the supplementary crystallographic data for this paper. These data can be obtained free of charge from The Cambridge Crystallographic Data Centre via www.ccdc.cam.ac.uk/data_request/cif.

1. *Annual Energy Review 2010 DOE/EIA-0384(2010)*, U.S. Energy Information Administration 2010.
2. *Electric Power Annual 2010*, US Energy Information Administration, November 9, 2011.
3. P. Denholm, E. Ela and B. Kirby, *The Role of Energy Storage with Renewable Electricity Generation*, NREL/TP-6A2-47187, 2010.
4. B. Dunn, H. Kamath and J.-M. Tarascon, *Science*, 2011, 334, 928 - 935.
5. Z. Yang, J. Zhang, M. C. W. Kintner-Meyer, X. Lu, D. Choi, J. P. Lemmon and J. Liu, *Chem. Rev.*, 2011, 111, 3577 - 3613.
6. A. Z. Weber, M. M. Mench, J. P. Meyers, P. N. Ross, J. T. Gostick and Q. Liu, *J. Appl. Electrochem.*, 2011, 41, 1137 - 1164.
7. W. Wang, Q. Luo, B. Li, X. Wei, L. Li and Z. Yang, *Adv. Funct. Mater.*, 2013, 23, 970 - 986.
8. L. Li, S. Kim, W. Wang, M. Vijayakumar, Z. Nie, B. Chen, J. Zhang, G. Xia, J. Hu, G. Graff, J. Liu and Z. Yang, *Adv. Energy Mater.*, 2011, 1, 394-400.
9. P. Alotto, M. Guarnieri and F. Moro, *Renew. Sust. Energ. Rev.*, 2014, 29, 325 - 335.
10. C. Ponce de León, A. Frías-Ferrer, J. González-García, D. A. Sźanto and F. C. Walsh, *J. Power Sources*, 2006, 160, 716 - 732.
11. S.-H. Shin, S.-H. Yun and S.-H. Moon, *RSC Adv.*, 2013, 3, 9095 - 9116.

12. L. E. Barrosse-Antle, A. M. Bond, R. G. Compton, A. M. O'Mahony, E. I. Rogers and D. S. Silvester, *Chem. Asian J.*, 2010, 5, 202-230.
13. Y. Matsuda, K. Tanaka, M. Okada, Y. Takasu and M. Morita, *J. Appl. Electrochem.*, 1988, 18, 909 - 914.
14. M. Morita, Y. Tanaka, K. Tanaka, Y. Matsuda and T. Matsumura-Inoue, *Bull. Chem. Soc. Jpn.*, 1988, 61, 2711 - 2714.
15. M. H. Chakrabarti, R. A. W. Dryfe and E. P. L. Roberts, *Electrochim. Acta*, 2007, 52, 2189 - 2195.
16. J.-H. Kim, K. J. Kim, M.-S. Park, N. J. Lee, U. Hwang, H. Kim and Y.-J. Kim, *Electrochem. Commun.*, 2011, 13, 997 - 1000.
17. J. Mun, M.-J. Lee, J.-W. Park, D.-J. Oh, D.-Y. Lee and S.-G. Doo, *Electrochem. Solid-State Lett.*, 2012, 15, A80 - A82.
18. Q. Liu, A. A. Shinkle, Y. Li, C. W. Monroe, L. T. Thompson and A. E. S. Sleightholme, *Electrochem. Commun.*, 2010, 12, 1634 - 1637.
19. Q. Liu, A. E. S. Sleightholme, A. A. Shinkle, Y. Li and L. T. Thompson, *Electrochem. Commun.*, 2009, 11, 2312 - 2315.
20. A. E. S. Sleightholme, A. A. Shinkle, Q. Liu, Y. Li, C. W. Monroe and L. T. Thompson, *J. Power Sources*, 2011, 196, 5742 - 5745.
21. T. Yamamura, Y. Shiokawa, H. Yamana and H. Moriyama, *Electrochim. Acta*, 2002, 48, 43 - 50.
22. D. Zhang, Q. Liu, X. Shi and Y. Li, *J. Power Sources*, 2012, 203, 201 - 205.
23. A. A. Shinkle, A. E. S. Sleightholme, L. D. Griffith, L. T. Thompson and C. W. Monroe, *J. Power Sources*, 2012, 206, 490 - 496.
24. A. A. Shinkle, A. E. S. Sleightholme, L. T. Thompson and C. W. Monroe, *J. Appl. Electrochem.*, 2011, 41, 1191 - 1199.
25. D. Zhang, H. Lan and Y. Li, *J. Power Sources*, 2012, 217, 199 - 203.
26. P. J. Cappillino, H. D. Pratt III, N. S. Hudak, N. C. Tomson, T. M. Anderson and M. R. Anstey, *Adv. Energy Mater.*, 2014, 4, 1.
27. H. D. Pratt III, N. S. Hudak, X. Fang and T. M. Anderson, *J. Power Sources*, 2013, 236, 259 - 264.
28. F. R. Brushett, J. T. Vaughey and A. N. Jansen, *Adv. Energy Mater.*, 2012, 2, 1390 - 1396.
29. Z. Li, S. Li, S. Liu, K. Huang, D. Fang, F. Wang and S. Peng, *Electrochem. Solid-State Lett.*, 2011, 14, A171 - A173.
30. W. Wang, W. Xu, L. Cosimbescu, D. Choi, L. Li and Z. Yang, *Chem. Commun.*, 2012, 48, 6669 - 6671.
31. M. Duduta, B. Ho, V. C. Wood, P. Limthongkul, V. E. Brunini, W. C. Carter and Y.-M. Chiang, *Adv. Energy Mater.*, 2011, 1, 511 - 516.
32. S. Hamelet, D. Larcher, L. Dupont and J.-M. Tarascon, *J. Electrochem. Soc.*, 2013, 160, A516 - A520.
33. S. Hamelet, T. Tzedakis, J.-B. Leriche, S. Sailler, D. Larcher, P.-L. Taberna, P. Simon and J.-M. Tarascon, *J. Electrochem. Soc.*, 2012, 159, A1360 - A1367.
34. M. Youssry, L. Madec, P. Soudan, M. Cerbelaud, D. Guyomard and B. Lestriez, *Phys. Chem. Chem. Phys.*, 2013, 15, 14476 - 14486.
35. X. Wei, L. Cosimbescu, W. Xu, J. Z. Hu, M. Vijayakumar, J. Feng, M. Y. Hu, X. Deng, J. Xiao, J. Liu, V. Sprenkle and W. Wang, *Adv. Energy Mater.*, 2014.
36. R. G. Charles, *Inorg. Syn.*, 1966, 8, 135 - 138.
37. J. P. Collman, R. L. Marshall, W. L. Young III and S. D. Goldby, *Inorg. Chem.*, 1962, 1, 704 - 710.
38. J. P.Collman, *Inorg. Syn.*, 1963, 7, 134 - 136.
39. K. B. Takvorian and R. B. Barker, *Inorg. Syn.*, 1970, 12, 85 - 88.
40. R. F. Handy and R. L. Lintvedt, *Inorg. Chem.*, 1974, 13, 893 - 896.
41. C. Tsiamis, C. C. Hadjikostas, S. Karageorgiou and G. Manoussakis, *Inorg. Chim. Acta*, 1988, 143, 17 - 23.
42. Z. Gu and A. Zakarian, *Org. Lett.*, 2010, 12, 4224.
43. *The authors note that the solubility measurements described herein are for the neutral complexes and that the solubility could significantly change upon changing the materials oxidation state. Future work will quantify the extent of this effect.*
44. *Polymorphism in materials 1 - 15 could have a significant effect on the solubility reported herein. In an effort to assess the extent of any changes in solid state packing the materials were assessed by powder X-ray diffraction (PXRD) prior to saturation and as the post saturation residues. In the cases were the materials were crystalline prior to saturation (1 - 9), a crystalline residue was obtained post-saturation. The highly soluble materials (10 - 13, 15) gave PXRD patterns consistent with amorphous solids both pre- and post-saturation.*
45. M. I. Pilo, *J. Electroanal. Chem.*, 1992, 323, 103 - 115.
46. X. Zhang, S. Wang and S. Qinghua, *Microchim. Acta*, 2005, 149, 37 - 42.
47. *This method is widely used to increase the resolution of redox reactions by generating a steady-state signal with peaks at the standard potential. This is done using the convolution theorem; the full derivation and examples are widely available.*
48. *One interesting characteristic of these cyclic voltammograms of 7-9 is that the couples resulting from ligand non-innocence have peak height ratios much closer to unity than the couples for chromium(III) acetylacetonate (1), indicating faster kinetics. Slow kinetics is detrimental to the operation of a flow battery and the incorporation of non-innocent ligands could be a way to overcome the kinetic limitations of chromium. The couples associated with the phenyl substituents also caused a negative voltage shift in the potentials of the redox couples relative to complex 1, which limits the number of couples within the stable voltage window.*
49. H. Ikeuchi, K. Naganuma, M. Ichikawa, H. Ozawa, T. Ino, M. Sato, H. Yonezawa, S. Mukaida, A. Yamamoto and T. Hashimoto, *J. Solution Chem.*, 2007, 36, 1243 - 1259.
50. I. L. Escalante-Garcia, J. S. Wainright, L. T. Thompson and R. F. Savinell, *Journal of Electrochemical Society*, 2014, (Submitted).
51. R. Auvergne, M.-H. Morel, P. Menut, O. Giani, S. Guilbert and J.-J. Robin, *Biomacromolecules*, 2008, 9, 664 - 671.
52. D. P. Shrout and D. A. Lightner, *Synthesis*, 1990, 11, 1062 - 1065.

Modulation of the ligand structure results in complex solubilities that can varied by more than four orders of magnitude. The most soluble of these complexes yields an electrolyte with theoretical energy densities 6-fold higher than commercial aqueous vanadium RFBs.